



# Photovoltaics: Life-cycle analyses

V.M. Fthenakis<sup>a,b,\*</sup>, H.C. Kim<sup>a</sup>

<sup>a</sup> Center for Life Cycle Analysis, Columbia University, New York, NY, USA

<sup>b</sup> Photovoltaic Environmental Research Center, Brookhaven National Laboratory, Upton, NY, USA

Received 2 October 2009; accepted 2 October 2009

Communicated by: Associate Editor Yogi Goswami

## Abstract

Life-cycle analysis is an invaluable tool for investigating the environmental profile of a product or technology from cradle to grave. Such life-cycle analyses of energy technologies are essential, especially as material and energy flows are often interwoven, and divergent emissions into the environment may occur at different life-cycle-stages. This approach is well exemplified by our description of material and energy flows in four commercial PV technologies, i.e., mono-crystalline silicon, multi-crystalline silicon, ribbon-silicon, and cadmium telluride. The same life-cycle approach is applied to the balance of system that supports flat, fixed PV modules during operation. We also discuss the life-cycle environmental metrics for a concentration PV system with a tracker and lenses to capture more sunlight per cell area than the flat, fixed system but requires large auxiliary components. Select life-cycle risk indicators for PV, i.e., fatalities, injuries, and maximum consequences are evaluated in a comparative context with other electricity-generation pathways.

© 2009 Elsevier Ltd. All rights reserved.

*Keywords:* Photovoltaics; Life-cycle analysis; Life-cycle assessment; Environmental and health effects; Energy payback times

## 1. Introduction

Photovoltaics (PV), made from semiconducting materials, convert photons into electricity. When sunlight hits these materials, photons with a certain wavelength trigger electrons to flow through the materials to produce direct current (DC) electricity. Commercial PV materials include multi-crystalline silicon, mono-crystalline silicon, amorphous silicon, and thin film technologies, such as cadmium telluride (CdTe), and copper indium diselenide (CIS). A typical PV system consists of the PV module and the balance of system (BOS) structures for mounting the PV modules and converting the generated electricity to alternate current (AC) electricity of the proper magnitude for usage in the power grid.

Life-cycle analysis (LCA) is a framework for considering the environmental inputs and outputs of a product or process from cradle to grave. It is employed to evaluate the environmental impacts of energy technologies, and the results are increasingly used in decisions about R&D funding and in formulating energy policies. Informational publications for decision-makers in the European Community (European Commission, 2003) and in Australia (Australian Coal Industry Association Research Program (ACARP), 2004) indicated that photovoltaics have relatively high environmental impacts compared with other technologies, e.g., greenhouse-gas (GHG) emissions of 180 g CO<sub>2</sub>-eq./kWh in Germany, and 100 g CO<sub>2</sub>-eq./kWh in Australia, 10 and 2.5 times higher than the GHG emissions of the nuclear-fuel cycle for each country, and 45% and 23% of those of combined cycle (CC) natural-gas power generation in the same country.

These impacts reflect the fossil-fuel-based energy used in producing the materials for solar cells, modules, and systems; however, the data used in these studies were outdated

\* Corresponding author. Address: Photovoltaic Environmental Research Center, Brookhaven National Laboratory, Upton, NY, USA.

E-mail address: [fthenakis@bnl.gov](mailto:fthenakis@bnl.gov) (V.M. Fthenakis).

## Nomenclature

a-Si	amorphous silicon	LPG	liquefied petroleum gas
AC	alternate current	mc-Si	multi-crystalline silicon
BOS	balance of system	mono-Si	mono-crystalline silicon
c-Si	crystalline silicon	NAICS	North American Industry Classification System
CdS	cadmium sulfide	NG	natural gas
CdTe	cadmium telluride	NO <sub>x</sub>	nitrogen oxide
CIGS	copper indium gallium selenide	PM	particulate matter
CIS	copper indium diselenide	PR	performance ratio
DC	direct current	PSA	probabilistic safety assessment
DNI	direct normal irradiance	PSI	Paul Scherrer Institute
EPBT	energy payback time	PV	photovoltaics
ESP	electrostatic precipitators	RMP	Risk Management Program
FBR	fluidized bed reactor	SiH <sub>4</sub>	silane
GaAs	gallium arsenide	SiHCl <sub>3</sub>	trichlorosilane
GHG	greenhouse gas	SO <sub>x</sub>	sulfur oxide
GWP	global warming potential	TeO <sub>2</sub>	tellurium dioxide
HCl	hydrogen chloride	TPE	thermoplastic elastomer
HCPV	high-concentration PV	UCTE	Union for the Coordination of Transmission of Electricity
HF	hydrogen fluoride	VTD	vapor transport deposition
LCA	life-cycle analysis (or assessment)		
LCI	life-cycle inventory		

and some assumptions made were invalid. In this paper we summarize the results of PV life-cycle analyses based on current data for three silicon and one thin-film technologies, emphasizing basic metrics including energy payback times (EPBTs), GHG emissions, criteria pollutant emissions, toxic metal emissions, human injuries and fatalities.

## 2. Previous studies

Previous life-cycle studies reported a wide range of primary energy consumption for Si-PV modules. Alsema reviewed such analyses from the 1990s and found considerable variance between investigators in their estimates of primary energy consumption (Alsema, 2000). Normalized per m<sup>2</sup>, the researchers reported 2400–7600 MJ of primary energy consumption for mc-Si, and 5300–16,500 MJ for mono-Si modules. Besides uncertainties in the data, he attributed these differences mainly to the assumptions and allocation rules that each author adopted for modeling the purification and crystallization stages of silicon. In those days, solar cells were mostly tailored from off-spec products of electronic-grade silicon not directly from solar-grade silicon, so that multiple allocation rules might well be applied to the energy and material inputs for each grade of silicon; currently, only 5% of solar cells are from off-spec electronic-grade silicon (Alsema, 2000; Alsema and de Wild-Scholten, 2005). Selecting only those process steps needed to produce solar-grade silicon, Alsema's own estimates were 4200 and 5700 MJ/m<sup>2</sup> for mc-Si and mono-Si modules, respectively (Alsema, 2000). These val-

ues correspond to an energy payback time (EPBT) of 2.5 and 3.1 years, and life-cycle greenhouse-gas emissions of 46 and 63 g CO<sub>2</sub>-eq./kWh for mc-Si PV with 13% efficiency and mono-Si with 14% efficiency, respectively, under Southern European (Mediterranean) conditions: insolation of 1700 kWh/m<sup>2</sup>/year, and a performance ratio of 0.75. The balance of system (BOS) components, such as a mounting support, a frame, and electrical components account for additional ~0.7 years of EPBT, and ~15 g CO<sub>2</sub>-eq./kWh of GHG emissions.

Meijer et al. (2003) more recently assessed a slightly higher energy expenditure of 4900 MJ/m<sup>2</sup> to produce an mc-Si module. They assumed that the 270-μm thick Si PV with 14.5% cell efficiency was fabricated from electronic-grade high-purity silicon, which entails greater energy consumption. Their corresponding EPBT estimate for the module was 3.5 years excluding BOS components; i.e., higher than Alsema's earlier determination of 2.5 years. The increase stems mainly from the low level of insolation in the Netherlands (1000 kWh/m<sup>2</sup>/year) compared with the average for Southern Europe (1700 kWh/m<sup>2</sup>/year), and, to a less degree, from the higher energy estimation for silicon (Alsema, 2000; Meijer et al., 2003). Jungbluth reported the life-cycle metrics of various PV systems under environmental conditions in Switzerland in 2000 (Jungbluth, 2005). He considered the environmental impacts for 300-μm thick multi- and mono-Si-PV module with 13.2% and 14.8% conversion efficiency, respectively. Depending on which of the two materials he evaluated, and their applications (i.e., façade, slanted roof, and flat

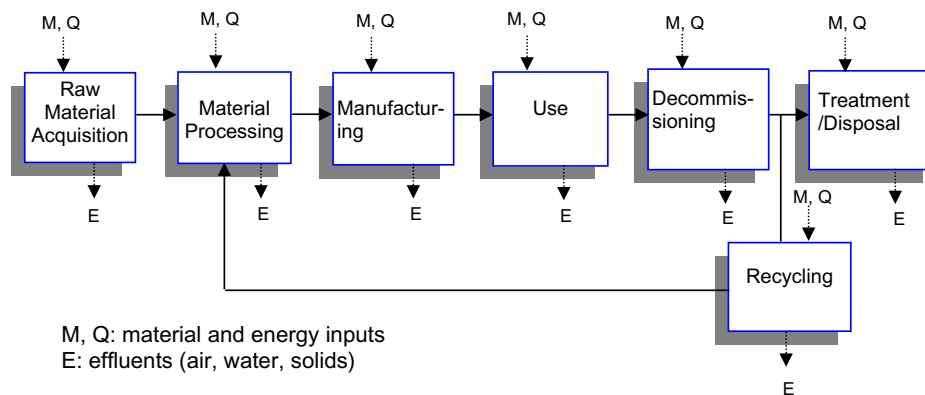


Fig. 1. Flow of the life-cycle stages, energy, materials, and wastes for PV systems.

roof), he arrived at figures of 39–110 g CO<sub>2</sub>-eq./kWh of GHG emissions and 3–6 years of EPBT for the average insolation of 1100 kWh/m<sup>2</sup>/year in that country. He assumed that the source of silicon materials was 50% from off-grade silicon and 50% from electronic-grade silicon, which is distant from the composition of the current (2005) PV supply (Alsema and de Wild-Scholten, 2005; Jungbluth, 2005).

There are fewer life-cycle studies of thin-film PV technologies; evaluations of the life-cycle primary energy consumption of amorphous silicon ranged between 710 and 1980 MJ/m<sup>2</sup> (Alsema, 2000). The differences are largely attributed to the choice of substrate and encapsulation materials. The lowest estimate, made by Palz and Zibetta (1991), considered a single glass structure, while the highest one by Hagedorn (1992) was based on a double-glass configuration to protect the active layer (Alsema, 2000; Palz and Zibetta, 1991). For CdTe PV, Hynes et al. (1994) based their energy analysis on two alternative technologies current at that time. The first employed non-vacuum electro-deposition of a 1.5- $\mu$ m absorber layer (CdTe), in conjunction with chemical-bath deposition of the 0.2- $\mu$ m window layer (CdS); the second method deposited both of these layers i.e.,  $\sim$ 5- $\mu$ m thick absorber layer and  $\sim$ 1.7- $\mu$ m thick window layer by thermal evaporation yielding. Their primary energy estimate for the first technology was 993 MJ/m<sup>2</sup>, and that for the second was 1188 MJ/m<sup>2</sup>. Kato et al.'s (2001) energy estimates were pertinent to the scale of annual production; they suggested that energy consumption will decline as the scale of production rises; they cited values of 1523, 1234, and 992 MJ/m<sup>2</sup> for frameless modules with annual capacities of 10, 30, and 100 MW<sub>p</sub>,<sup>1</sup> respectively. However, these earlier estimates fall far short of describing present-day commercial-scale CdTe PV production that, unlike previously, now encompasses many large-scale production plants.

### 3. Life cycle of photovoltaics

The life-cycle stages of photovoltaics involve (1) the production of raw materials, (2) their processing and purification, (3) the manufacture of modules and balance of system (BOS) components, (4) the installation and use of the systems, and (5) their decommissioning and disposal or recycling (Fig. 1).

Production starts with mining the raw materials (i.e., quartz sand for silicon PV; Zn- and Cu-ores for CdTe PV), and continues with their processing and purification (Fig. 2) (Fthenakis et al., 2008). The silica in the quartz sand is reduced in an arc furnace to metallurgical-grade silicon, which must be purified further into “electronic-grade” or “solar-grade” silicon, typically through a “Siemens” process. Crystalline silicon modules typically are framed for additional strength and easy mounting. The recent LCAs for crystalline silicon are based on life-cycle inventory (LCI) data provided, collectively, by eleven European and US photovoltaic companies participating in the European Commission’s Crystal Clear project. The data sets were published in separate papers by Alsema and de Wild-Scholten (2005) and by Fthenakis and Alsema (2006).

The life-cycle inventories of the minor metals used in thin-film PVs such as Cd, In, Mo, and Se, are closely related to the production cycle of base metals (Zn, Cu). The allocations of emissions and energy use between the former and the latter during mining, smelting and refining stages are described elsewhere (Fthenakis et al., 2009). Fthenakis (2004) described the material flows of cadmium (Cd) and emissions from the entire life-cycle stages of cadmium telluride (CdTe) PV. The life cycle starts with the production of Cd and Te that are byproducts, respectively, of smelting Zn- and Cu-ores (Fig. 2). Cd is obtained from the Zn waste streams, such as particulates collected in air-pollution-control equipment, and slimes collected from Zn-electrolyte purification stages. Cadmium is further processed and purified to meet the four or five 9 s purity required for synthesizing CdTe. Te is recovered and extracted after treating the slimes produced during electrolytic copper refining with dilute sulfuric acid; these slimes

<sup>1</sup> Peak power.

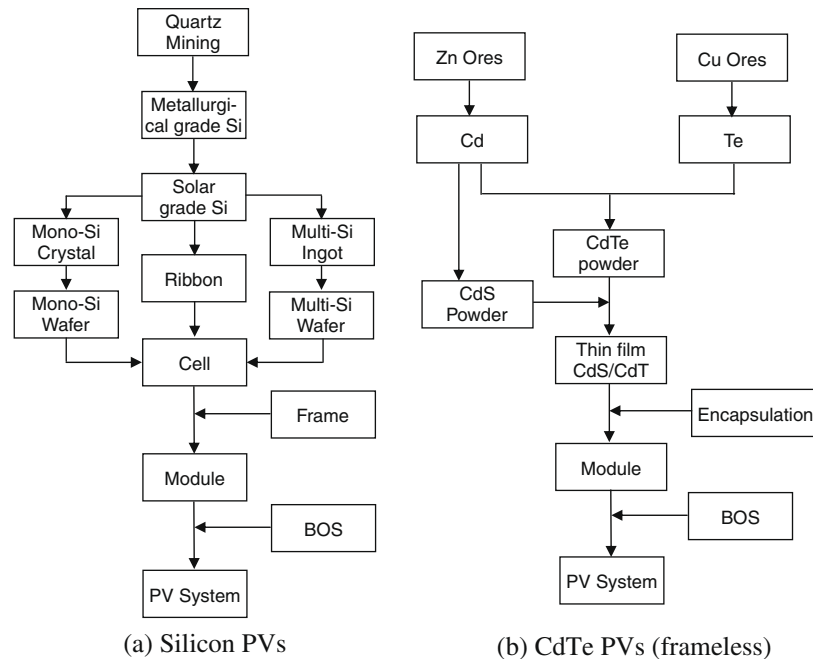


Fig. 2. Detailed flow diagram from the raw material acquisition to manufacturing stage of PVs (Fthenakis et al., 2008).

also contain Cu, and other metals. After cementation with copper, CuTe is leached with caustic soda to produce a sodium-telluride solution that is used as the feed for Te and TeO<sub>2</sub>. Additional leaching and vacuum distillation gives Cd and Te powders of semiconductor grade (i.e., 99.999%).

## 4. Life-cycle inventory

### 4.1. Modules

The material and energy inputs and outputs during the life cycles of Si PVs, viz., ribbon-Si, multi-Si, mono-Si, and also thin-film CdTe PV, were investigated in detail based on actual measurements from PV production plants between 2004 and 2006. Alsema and de Wild-Scholten recently updated the life-cycle inventory (LCI) for the technology for producing crystalline silicon modules in Western Europe under the framework of the Crystal Clear

project; a large European Integrated Project focusing on crystalline silicon technology, co-funded by the European Commission and the participating countries (Alsema and de Wild-Scholten, 2005; de Wild-Scholten and Alsema, 2005). Fthenakis and Kim reported the LCI data for CdTe thin-film technology taken from the production data from First Solar's plant in Perrysburg, Ohio, United States (Fthenakis and Kim, 2005). Table 1 presents the simplified life-cycle inventories (LCI) for 2006, compiled from the data from eleven European and two US plants along with values in the literature of Alsema and de Wild-Scholten (2005) and Fthenakis and Kim (2005).

The typical thickness of multi- and mono-Si PV is 270–300 μm, and that of ribbon-Si is 300–330 μm; 72 individual cells of 156 cm<sup>2</sup> (125 cm × 125 cm) comprise a module of 1.25 m<sup>2</sup> for all Si-PV types. The conversion efficiency of ribbon-, multi-, and mono-Si module is 11.5%, 13.2%, and 14.0%, respectively. On the other hand, as of 2006, First Solar's 25-MW<sub>p</sub> plant manufactures frameless,

Table 1  
Materials and energy inputs for PV systems to produce 1 m<sup>2</sup> of module including process loss, updated for 2006 (excluding the frame for Si modules).

Category	Inputs	Ribbon-Si	Multi-Si	Mono-Si	CdTe
Components (kg)	Cell materials	0.9	1.6	1.5	0.065
	Glass	9.1	9.1	9.1	19.2
	Ethylene vinyl acetate	1.0	1.0	1.0	0.6
	Others	1.8	1.8	1.8	2.0
Consumables (kg)	Gases	6.1	2.2	7.8	0.001
	Liquid	2.2	6.8	6.6	0.67
	Others	0.01	4.3	4.3	0.4
Energy	Electricity (kWh)	182	248	282	59
	Oil (l)	0.05	0.05	0.05	0.05
	Natural gas (MJ)	166	308	361	–

double-glass, CdTe modules of 1.2 m by 0.6 m, rated at 9% photon-to-electricity conversion efficiency with  $\sim 3\text{-}\mu\text{m}$  thick active layer.

The data for Si PVs extend from the production stage of solar-grade Si to the module manufacturing stage, while those for CdTe PV correspond to the deposition of the CdTe film and the module's manufacturing stages. The metallurgical-grade silicon that is extracted from quartz is purified into solar-grade polysilicon by either a silane ( $\text{SiH}_4$ ) or trichlorosilane ( $\text{SiHCl}_3$ )-based process. The energy requirement for this purification step is the most important demand for crystalline Si-PV modules, accounting for 45% of the primary energy used for fabricating multi-Si modules. Two technologies are currently employed for producing polysilicon from silicon gases: the Siemens reactor method and the fluidized bed reactor (FBR) method. In the former, which accounts for the majority ( $\sim 90\%$  in 2004) of solar-grade silicon production in the US, silane- or trichlorosilane-gas is introduced into a thermal decomposition furnace (reactor) with high temperature ( $\sim 1100\text{--}1200\text{ }^\circ\text{C}$ ) polysilicon rods (Aulich and Schulze, 2002; Woditsch and Koch, 2002; Maycock, 2005). The silicon rods grow as silicon atoms in the gas deposit onto them, up to 150 mm in diameter and up to 150 cm in length (Aulich and Schulze, 2002). The data on Si PVs in Table 1 are based on averages over standard and modified Siemens reactors. The former primarily produces the electronic-grade silicon with a purity of over nine 9 s, while the latter produces the solar-grade silicon with a purity of six to eight 9 s, consuming less energy than the former (Williams, 2000). The scenario involving the scrap silicon from electronic-grade silicon production is not considered as the market share of this material accounts for only 5% in 2005 (Rogol, 2005).

#### 4.2. Balance of system (BOS)

Little attention has been paid to the LCA studies of the balance of system (BOS), and so inventory data are scarce. Depending on the application, solar cells are either rooftop- or ground-mounted, both operating with a proper balance of system (BOS). Silicon modules need an aluminum frame of  $3.8\text{ kg/m}^2$  for structural robustness and easy installation, while a glass backing performs the same functions for the CdTe PV produced in the US (Alsema and de Wild-Scholten, 2005; Fthenakis and Kim, 2005). For a rooftop PV application, the BOS typically includes inverters, mounting structures, cable and connectors. Large-scale ground-mounted PV installations require additional equipment and facilities, such as grid connections, office facilities, and concrete.

A recent analysis of a 3.5 MW<sub>p</sub> mc-Si installation at the Springerville Generating Station in Arizona affords a detailed materials- and energy balance for a ground-mounted BOS (Table 2) (Mason et al., 2006). For this study, Tucson Electric Power (TEP) prepared the BOS bill of materials- and energy-consumption data for their mc-Si-

Table 2

Mass balance of major components for the 3.5 MW Tucson Electric Power generating plant in Springerville, AZ, based on 30 years of operation.

Balance of system	Mass (kg/MW <sub>p</sub> )	% of total
<i>BOS</i>		
PV support structure	16,821	10.3
Module interconnections	453	0.3
Junction boxes	1385	0.8
Conduits and fittings	6561	4.0
Wire and grounding devices	5648	3.4
Inverters and transformers	28,320	17.3
Grid connections	1726	1.1
Office facilities	20,697	12.6
Concrete	76,417	46.6
Miscellaneous	5806	3.5
Total	163,834	100.0
Frame <sup>a</sup>	18,141	

<sup>a</sup> Based on 12.2% rated efficiency for mc-Si module.

PV installations. The life expectancy of the PV metal support structures is assumed to be 60 years. Inverters and transformers are considered to last for 30 years, but parts must be replaced every 10 years, amounting to 10% of their total mass, according to well-established data from the power industry on transformers and electronic components. The inverters are utility-scale, Xantrec PV-150 models with a wide-open frame, allowing failed parts to be easily replaced. The life-cycle inventory includes the office facility's materials and energy use for administrative, maintenance, and security staff, as well as the operation of maintenance vehicles. Aluminum frames are shown separately, since they are part of the module, not of the BOS inventory; there are both framed and frameless modules on the market.

de Wild-Scholten et al. (2006) studied two classes of rooftop-mounting systems based on a mc-Si-PV system called SolarWorld SW220 with dimensions of  $1001\text{ mm} \times 1675\text{ mm}$ , 220 W<sub>p</sub>; they are used for on-roof mounting where the system builds on existing roofing material, and in-roof mounting where the modules replace the roof tiles. The latter case is credited in terms of energy and materials use because roof tile materials then are not required. Table 3 details the LCI of several rooftop-mounting systems, cabling, and inverters. Two types (500 and 2500 W) of small inverters adequate for rooftop PV design were inventoried. A transformer is included as an electronic component for both models. The amount of control electronics will become less significant for inverters with higher capacity ( $>10\text{ kW}$ ), resulting in less material use per PV capacity (de Wild-Scholten et al., 2006).

## 5. Energy payback times and greenhouse-gas emissions

### 5.1. Energy payback time

The most frequently measured life-cycle metrics for PV system environmental analyses are the energy payback time

Table 3  
LCI of balance of system (BOS) for rooftop mounting (de Wild-Scholten and al., 2006).

	On-roof		In-roof	
	Phönix, TectoSun	Schletter, Eco05 + EcoG	Schletter, Plandach 5	Schweizer, Solrif
<i>(a) Mounting system (kg/m<sup>2</sup>)</i>				
Low alloy steel	0	0	0	0
Stainless steel	0.49	0.72	0.28	0.08
Aluminum	0.54	0.97	1.21	1.71
Concrete	0	0	0	0
Frame	3.04	0	0	0
<i>(b) Cabling (g/m<sup>2</sup>)</i>				
		Helukabel, Solarflex 101, 4 mm <sup>2</sup> , DC		Helukabel, NYM-J, 6 mm <sup>2</sup> , AC
Copper		83.0		19.9
Thermoplastic elastomer (TPE)		64.0		0.0
PVC		0.0		16.9
<i>(c) Inverters (g)</i>				
		Philips PSI 500 (500 W)		Mastervolt SunMaster 2500 (2500 W)
Steel		78		9800
Aluminum		682		1400
Copper		2		
Polycarbonate		68		
ABS		148		
Other plastics		5.4		
Printed circuit board		100		1800 <sup>a</sup>
Connector		50		
Transformers, wire-wound		310		5500
Coils		74		
Transistor diode		10		
Capacitor, film		72		
Capacitor, electrolytic		54		
Other electric components		20		

<sup>a</sup> Including electric components.

(EPBT) and the greenhouse-gas (GHG) emissions. Energy payback time is defined as the period required for a renewable energy system to generate the same amount of energy (either primary or kWh equivalent) that was used to produce the system itself.

Energy Payback Time(EPBT)

$$= (E_{mat} + E_{manuf} + E_{trans} + E_{inst} + E_{EOL}) / (E_{agen} - E_{aoper})$$

where  $E_{mat}$ , primary energy demand to produce materials comprising PV system;  $E_{manuf}$ , primary energy demand to manufacture PV system;  $E_{trans}$ , primary energy demand to transport materials used during the life cycle;  $E_{inst}$ , primary energy demand to install the system;  $E_{EOL}$ , primary energy demand for end-of-life management;  $E_{agen}$ , annual electricity generation in primary energy term;  $E_{aoper}$ , annual energy demand for operation and maintenance in primary energy term.

Calculating the primary energy equivalent requires knowledge of the country-specific, energy-conversion parameters for fuels and technologies used to generate energy and feedstock. The annual electricity generation ( $E_{agen}$ ) is represented as primary energy based on the efficiency of electricity conversion at the demand side. The electricity is converted to the primary energy term by the

average conversion efficiency of 0.29 for the United States and 0.31 for Western Europe (Dones et al., 2003; Franklin Associates, 1998).

## 5.2. Greenhouse-gas emissions

The greenhouse-gas (GHG) emissions during the life-cycle stages of a PV system are estimated as an equivalent of CO<sub>2</sub> using an integrated time horizon of 100 years; the major emissions included as GHG emissions are CO<sub>2</sub> (GWP<sup>2</sup> = 1), CH<sub>4</sub> (GWP = 23), N<sub>2</sub>O (GWP = 296), and chlorofluorocarbons (GWP = 4600–10,600) (International Panel on Climate Change, 2001). Electricity and fuel use during the PV materials and module production are the main sources of the GHG emissions for PV cycles. Upstream electricity-generation methods also play an important role in determining the total GHG emissions. For instance, the GHG emission factor of the average US electricity grid is 40% higher than that of the average

<sup>2</sup> Global warming potential, indicator of the relative radiative effect of a substance compared to CO<sub>2</sub>, integrated over a chosen time horizon 25. Intergovernmental Panel on Climate Change, Climate Change 2001: The Scientific Basis, 2001, Cambridge, UK: Cambridge University Press.

Western European (UCTE) grid although emission factors of fossil-fuel combustion are similar, resulting in higher GHG estimates for the US - produced modules (Dones et al., 2003; Franklin Associates, 1998).

With material-inventory data from industry, Alsema and de Wild-Scholten (2005) demonstrated that the life-cycle primary energy and greenhouse-gas emissions of complete rooftop Si-PV systems are much lower than those reported in earlier studies. Primary energy consumption is 2300, 3700, and 4200 MJ/m<sup>2</sup>, respectively, for ribbon-, multi-, and mono-Si modules. Fthenakis and Alsema also report that the GHG emissions of Si modules corresponding to 2004–2005 production are within a 30–45 g CO<sub>2</sub>-eq./kWh range, with an EPBT of 1.7–2.7 years for a rooftop application under Southern European insolation of 1700 kWh/m<sup>2</sup>/year and a performance ratio<sup>3</sup> (PR) of 0.75 (Figs. 3 and 4, respectively) (Alsema and de Wild-Scholten, 2005; Fthenakis and Alsema, 2006). We note that in these estimates, the BOS for rooftop application accounts for 4.5–5 g CO<sub>2</sub>-eq./kWh of GHG emissions and 0.3 years of EPBT. These calculations were based on the electricity mixture for the current production of Si, within the context of the Crystal Clear project. For CdTe PV, we estimate the energy consumption 1200 MJ/m<sup>2</sup>, based on the actual production data of the year 2005 from the First Solar's 25 MW<sub>p</sub> plant in Ohio, United States, close to the early studies reviewed (Hynes et al., 1994; Kato et al., 2001). The greenhouse-gas (GHG) emissions and energy payback time (EPBT) of ground-mounted CdTe PV modules under the average US insolation condition, 1800 kWh/m<sup>2</sup>/year, were determined to be 24 g CO<sub>2</sub>-eq./kWh and 1.1 years, correspondingly. These estimates include 6 g CO<sub>2</sub>-eq./kWh of GHG and 0.3 year of EPBT contribution from the ground-mounted BOS (Fthenakis and Kim, 2005). On the other hand, Raugei et al. (2007) estimates a lower primary energy consumption, ~1100 MJ/m<sup>2</sup>, and thereby less GHG emissions and lower EPBT than ours, based on the data of the year 2002 from the Antec Solar's 10 MW<sub>p</sub> plant in Germany (Figs. 3 and 4). The source of the difference between the two estimates is yet to be studied.

We note that this picture is not a static one and expect that improvements in material and energy utilization and recycling will continue to improve the environmental profiles. A recent, major improvement is a recycling process for the sawing slurry, the cutting fluid that is used in the wafer cutting (Alsema et al., 2006). This recycling process recovers 80–90% of the silicon carbide and polyethylene glycol which used to be wasted. As we show in Fig. 4, recycling silicon carbide and polyethylene glycol from silicon slurries decreases the EPBTs of these technologies by 10%. On the other hand, any increases in the electric-conversion efficiencies of the modules will entail a proportional

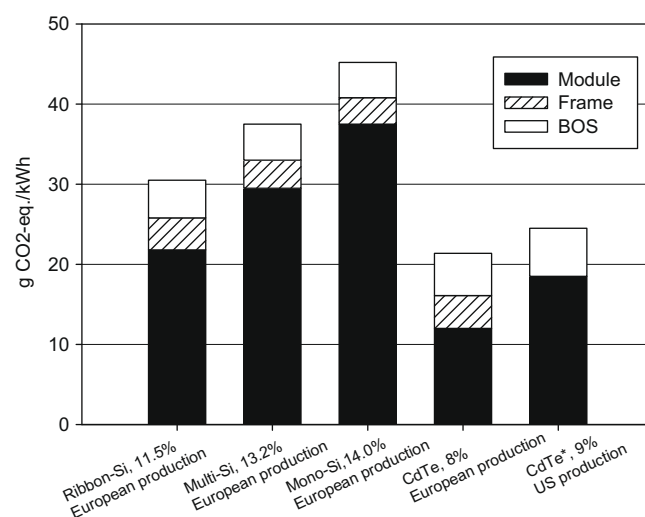


Fig. 3. Life-cycle GHG emissions from silicon and CdTe PV modules, wherein BOS is the balance of system, that is the module's supports, cabling and power conditioning (Alsema et al., 2005; Fthenakis et al., 2004; Wild-Scholten et al., 2005; Fthenakis et al., 2005; Raugei et al., 2007). Unless otherwise noticed, the estimates are based on rooftop-mount installation, Southern European insolation, 1700 kWh/m<sup>2</sup>/year, a performance ratio of 0.75, a lifetime of 30 years. \*Based on ground-mount installation, average US insolation of 1800 kWh/m<sup>2</sup>/year, and a performance ratio of 0.8.

improvement of the EPBT. Fig. 5 compares these emissions with those of conventional fuel-burning power plants, revealing the considerable environmental advantage of PV technologies. The majority of GHG emissions are from the operation stage for the coal, natural gas, and oil fuel cycles while the material and device production accounts for nearly all the emissions for the PV cycles. The GHG emissions from the nuclear-fuel cycle are mainly related to the fuel production, i.e., mining, milling, fabrication, conversion, and enrichment of uranium fuel. The details of the US nuclear-fuel cycle is described elsewhere (Fthenakis and Kim, 2007a).

## 6. Criteria pollutant and heavy metal emissions

### 6.1. Criteria pollutant emissions

The emissions of criteria pollutants during the life cycle of a PV system are largely proportional to the amount of fossil fuel burned during its various phases, in particular, PV material processing and manufacturing; therefore, the emission profiles are close to those of the greenhouse-gas emissions (Fig. 6). Toxic gases and heavy metals can be emitted directly from material processing and PV manufacturing, and indirectly from generating the energy used at both stages. Accounting for each of them is necessary to create a complete picture of the environmental impact of a technology. An interesting example of accounting for the total emissions is that of cadmium flows in CdTe and other PV technologies, as discussed next.

<sup>3</sup> Ratio between the ideal and actual electricity output.

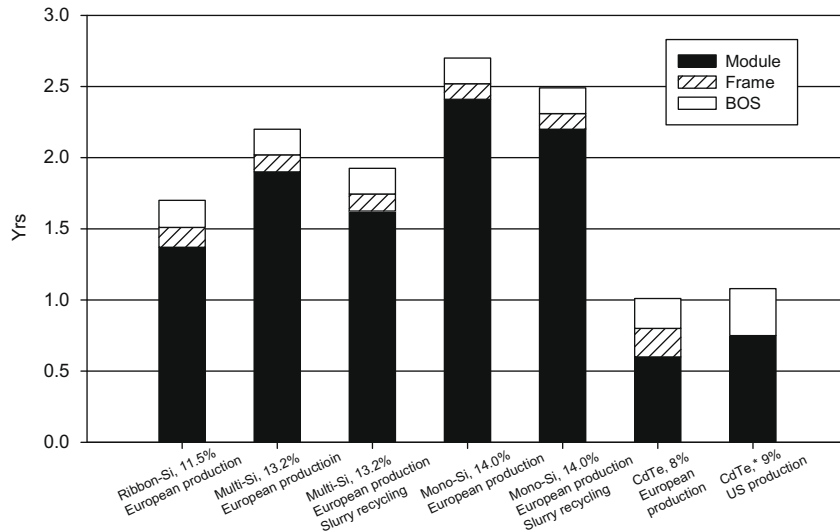


Fig. 4. Energy payback time for silicon and CdTe PV modules, wherein BOS is the balance of system, that is the module supports, cabling and power conditioning (Alsema et al., 2005; Fthenakis et al., 2004; Wild-Scholten et al., 2005; Fthenakis et al., 2005; Rauegi et al., 2007; Alsema et al., 2006). Unless otherwise noticed, the estimates are based on rooftop-mount installation, Southern European insolation, 1700 kWh/m<sup>2</sup>/year, a performance ratio of 0.75, and a lifetime of 30 years. \*Based on ground-mount installation, average US insolation of 1800 kWh/m<sup>2</sup>/year, and a performance ratio of 0.8.

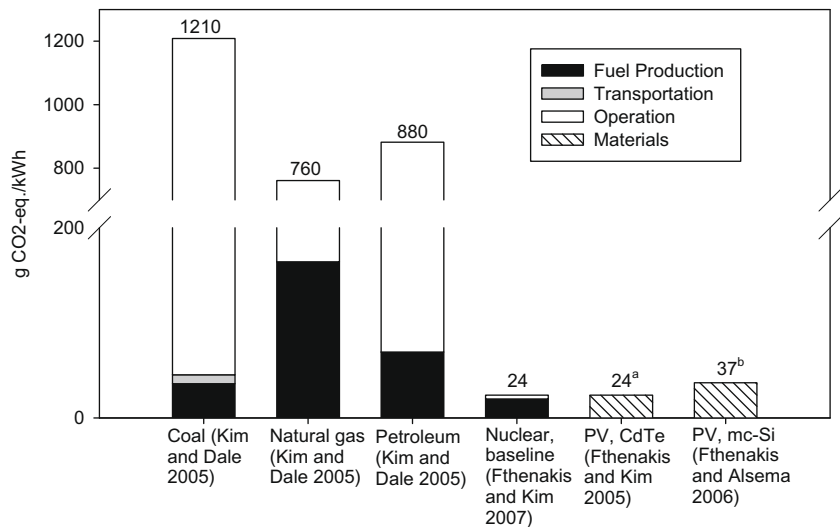


Fig. 5. Comparison of GHG emissions from PV with those from conventional power plants (<sup>a</sup>based on the average US insolation, 1800 kWh/m<sup>2</sup>/year and a performance ratio of 0.8; <sup>b</sup>based on the Southern European insolation, 1700 kWh/m<sup>2</sup>/year and a performance ratio of 0.75).

## 6.2. Heavy metal emissions

### 6.2.1. Direct emissions

Cadmium is a byproduct of zinc and lead, and is collected from emissions and waste streams during the production of these major metals. The largest fraction of cadmium, with ~99.5% purity, is in the form of a sponge from the electrolytic recovery of zinc. This sponge is transferred to a cadmium-recovery facility, and is further processed through oxidation and leaching to generate a new electrolytic solution. After selectively precipitating the major impurities, cadmium of 99.99% purity is recovered by electrowinning. It is further purified by vacuum distillation to the five 9s purity required for CdTe PV

manufacturing. The emissions during each of these steps are detailed elsewhere (Fthenakis, 2004). They total up to 0.02 g per GWh of PV-produced energy under Southern European condition (Table 4). On the other hand, cadmium emissions during the lifespan of a finished CdTe module are negligible; the only conceivable pathway of release is if a fire broke out. Experiments at Brookhaven National Laboratory that simulated real fire conditions revealed that CdTe is effectively contained within the glass-to-glass encapsulation during the fire, and only minute amounts (0.4–0.6%) of Cd are released. The dissolution of Cd into the molten glass was confirmed by high-energy synchrotron X-ray microscopy (Fthenakis et al., 2005).

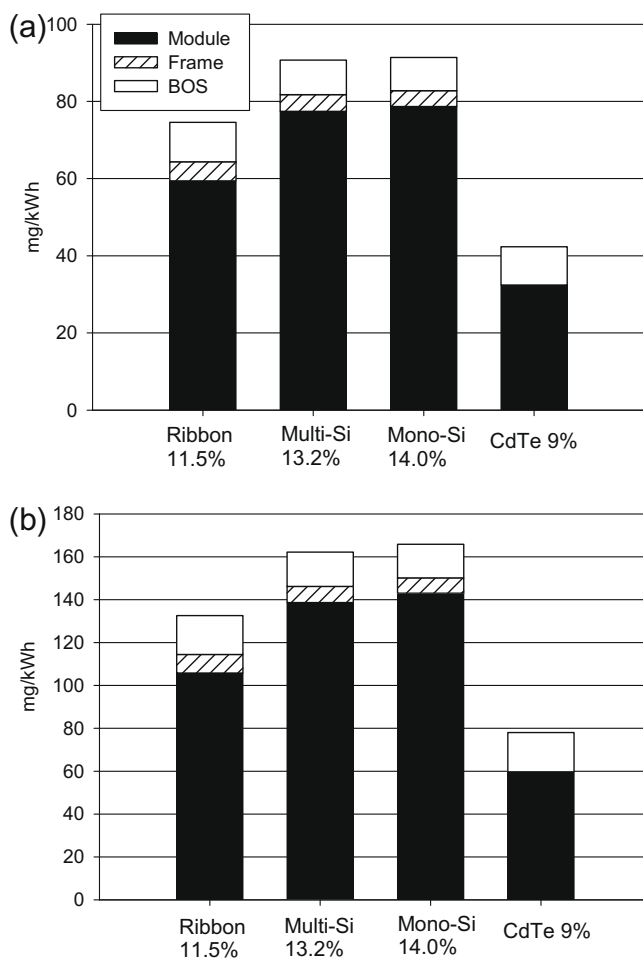


Fig. 6. Life-cycle emissions of (a) NO<sub>x</sub>, and (b) SO<sub>x</sub> emissions from silicon and CdTe PV modules, wherein BOS is the balance of system, that is module supports, cabling and power conditioning. The estimates are based on rooftop-mount installation, Southern European insolation, 1700 kWh/m<sup>2</sup>/year, a performance ratio of 0.75, and a lifetime of 30 years. It is assumed that the electricity supply for all the PV system is from the UCTE grid.

### 6.2.2. Indirect emissions

Coal and oil-fired power plants routinely generate Cd during their operation, as it is a trace element in both fuels. According to the US Electric Power Research Institute's (EPRI's) data, under the best/optimized operational and maintenance conditions, burning coal for electricity releases into the air between 2 and 7 g of Cd/GWh (Electric Power Research Institute (EPRI), 2002). In addition, 140 g/GWh of Cd inevitably collects as fine dust in boilers, bag-houses, and electrostatic precipitators (ESPs). Furthermore, a typical US coal-powered plant emits per GWh about 1000 tons of CO<sub>2</sub>, 8 tons of SO<sub>2</sub>, 3 tons of NO<sub>x</sub>, and 0.4 tons of particulates. The emissions of Cd from heavy-oil burning power plants are 12–14 times higher than those from coal plants, even though heavy oil contains much less Cd than coal (~0.1 ppm), because these plants do not have particulate-control equipment. Cadmium emissions also are associated with natural gas and

Table 4

Direct, atmospheric Cd emissions during the life cycle of the CdTe PV module (allocation of emissions to co-production of Zn, Cd, Ge and In).

	Air emissions (g Cd/tonne Cd <sup>a</sup> )	Allocation (%)	Air emissions (g Cd/tonne Cd <sup>a</sup> )	mg Cd/GWh <sup>b</sup>
Mining of Zn ores	2.7	0.58	0.016	0.02
Zn smelting/refining	40	0.58	0.23	0.3
Cd purification	6	100	6	9.1
CdTe production	6	100	6	9.1
PV manufacturing	3	100	3	4.5
Operation	0.3	100	0.3	0.3
Disposal/recycling	0	100	0	0
Total			15.55	23.3

<sup>a</sup> Tonne of Cd produced.

<sup>b</sup> Energy produced assuming average Southern European insolation (i.e., 1700 kWh/m<sup>2</sup>/yr), 9% electrical-conversion efficiency, and a 30-year life for the modules.

nuclear-fuel life cycles because of the energy used in the associated fuel processing and material productions (Dones et al., 2003).

We accounted for Cd emissions in generating the electricity used in producing a CdTe PV system (Fthenakis and Kim, 2007b). The assessment of electricity demand for PV modules and BOS was based on the life-cycle inventory of each module and the electricity input data for producing BOS materials. Then, Cd emissions from the electricity demand for each module were assigned, assuming that the life-cycle electricity for the silicon- and CdTe-PV modules was supplied by the UCTE grid. The indirect Cd emissions from electricity usage during the life cycle of CdTe PV modules (i.e., 0.24 g/GWh) are an order-of-magnitude greater than the direct ones (routine and accidental) (i.e., 0.02 g/GWh).

The complete life-cycle atmospheric Cd emissions, estimated by adding those from the electricity and fuel demand associated with manufacturing and materials production for various PV modules and balance of system (BOS), are compared with the emissions from other electricity-generating technologies (Fig. 7) (Fthenakis et al., 2008). Undoubtedly, displacing the others with CdTe PV markedly lowers the amount of Cd released into the air. Thus, every GWh of electricity generated by CdTe PV modules can prevent around 5 g of Cd air emissions if they are used instead of, or as a supplement to, the UCTE electricity grid. Also, the direct emissions of Cd during the life cycle of CdTe PV are 10 times lower than the indirect ones due to electricity and fuel use in the same life cycle, and about 30 times less than those indirect emissions from crystalline photovoltaics. Furthermore, we examined the indirect heavy metal emissions in the life cycle of the three silicon technologies discussed earlier, finding that, among PV technologies, CdTe PV with the lowest energy payback time has the fewest heavy metal emissions (Fig. 8) (Fthenakis et al., 2008).

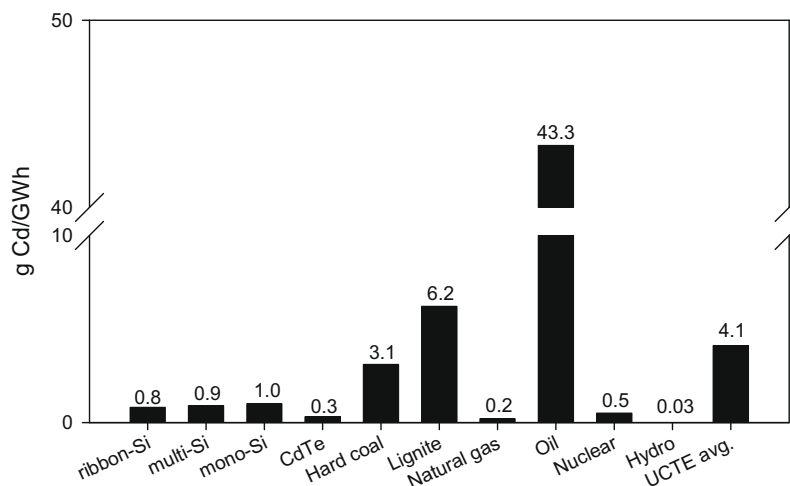


Fig. 7. Life-cycle atmospheric Cd emissions for PV systems from electricity and fuel consumption, normalized for a Southern European average insolation of 1700 kWh/m<sup>2</sup>/yr, performance ratio of 0.8, and lifetime of 30 years. A ground-mounted BOS is assumed for all PV systems (Fthenakis et al., 2008).

## 7. Concentrator PV systems

### 7.1. Overview

The primary purpose for establishing concentrating PV systems is to capture the maximum amount of sunlight and focus it on to a small cell area, thereby ultimately reducing the cost of high-efficiency solar-cell materials. For example, the commercialization of III–V multi-junction solar cells that originally were designed for space application is expanding via combination with concentrators (Swanson, 2003; Peharz and Dimroth, 2005). As the optics of concentrator modules capture only direct solar illumination, they must move to track the sun's trajectory during the day. Single- or two-axis trackers with hydraulic

drives, light sensors, and controllers are the commonest configuration.

We conducted an LCA for one of the most promising concentrator designs, the Amonix high-concentrator PV (HCPV) system (Fig. 9) (Kim and Fthenakis, 2006). This system consists of units called MegaModules mounted on two-axis trackers. Each MegaModule consists of 48 blocks of sub-module units, rated at 4.8 kW<sub>p</sub>-ac each under 850 W/m<sup>2</sup> of direct normal irradiance (DNI). A refractive concentration technology based on acrylic Fresnel lenses achieves an effective concentration ratio of 250. Each piece of thin acrylic plate with 24 lenses, 4-mm thick and anti-reflection coated, is mounted on each sub-module. A total of 1152 single-junction, single-crystal silicon cells, each 1.2 cm<sup>2</sup>, are mounted at the focal points of a MegaModule.

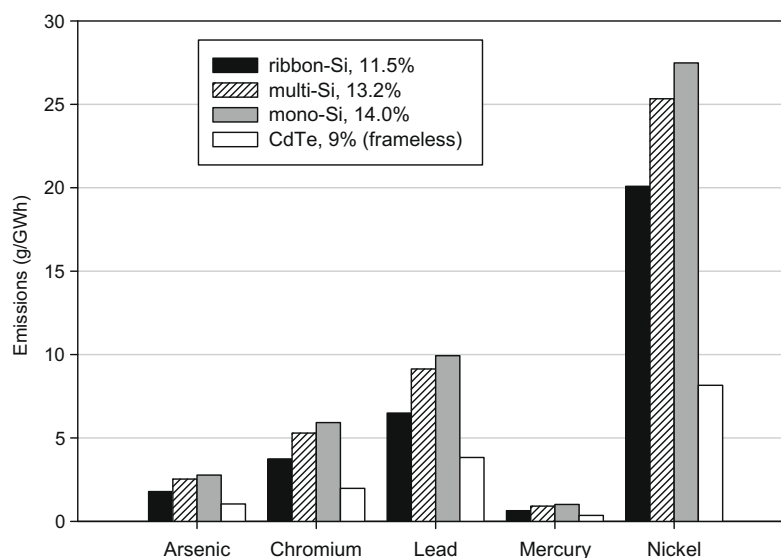


Fig. 8. Emissions of heavy metals from PVs due to electricity use, based on UCTE grid mix. Emissions are normalized for Southern European average insolation of 1700 kWh/m<sup>2</sup>/year, performance ratio of 0.8, and lifetime of 30 years. Each PV system is assumed to include a ground-mounted BOS as described by Mason et al. (2006).

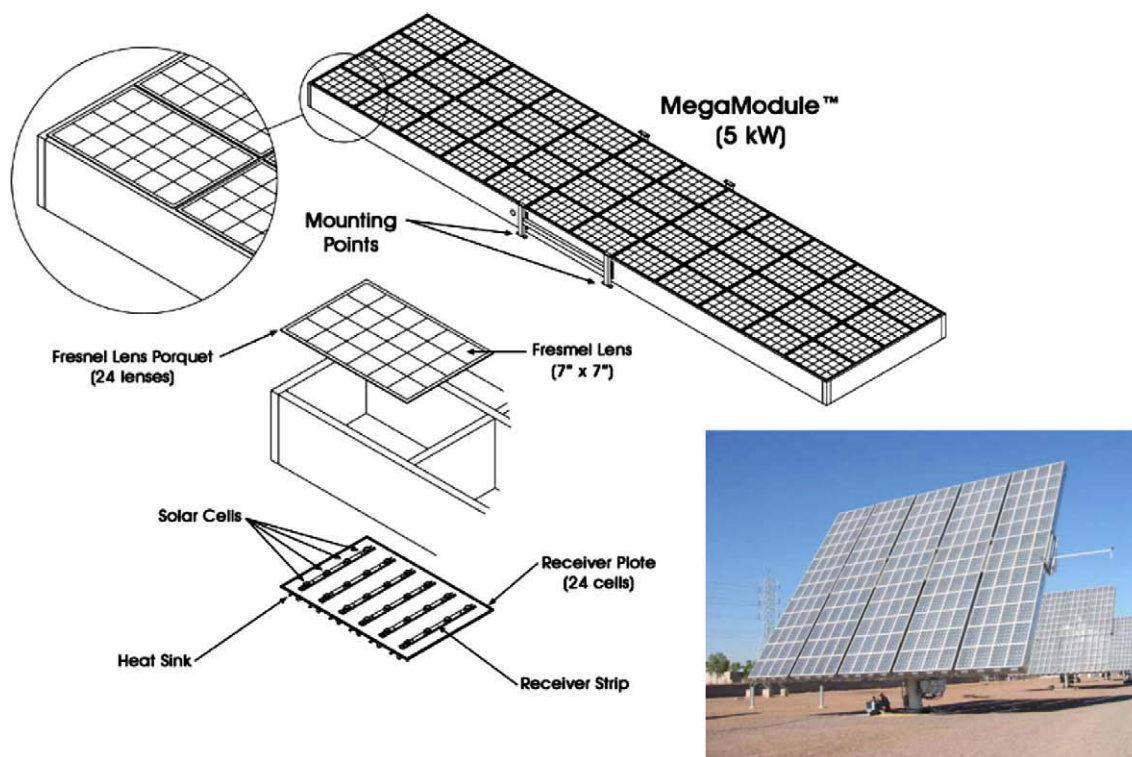


Fig. 9. Details of MegaModule in Amonix HCPV system, and complete 24 kW systems in APS STAR center in Phoenix ([www.amonix.com](http://www.amonix.com)).

This AM-10™ single-crystal solar cell operates at 26.5% efficiency (Garboushian et al., 1997). Arizona Public Service (APS) has installed and tested several Amonix HCPV systems with capacities of around 500 kW<sub>p</sub>, the largest being the 168 kW<sub>p</sub> installation at their PV plant near Prescott, Arizona.

The major components of this 5-MegaModule, 24 kW<sub>p</sub> system include frames, optics, single-crystal Si cells, heat sinks, tracker, foundation, hydraulic drive, motor, controller, inverter, sensor, power meter, and anemometer. While the aperture area is 182 m<sup>2</sup>, the total area of the concentrator is 230 m<sup>2</sup> including frame areas. The tracker consists of a 5.5 m high pedestal, a torque tube and a hydraulic drive with a controller. The concrete foundation used in the STAR test facility in Phoenix, from where the data for this analysis were taken, is 5.5 m deep and 1.2 m in diameter. Each 24 kW<sub>p</sub> MegaModule system has a 30 kW Xantrex inverter and multiple MegaModules share one transformer.

The direct beam solar radiation for concentrating collectors with a two-axis is, on average, 2480 kWh/m<sup>2</sup>/year in Phoenix, AZ (NREL, 1994). Performing with 16% rated AC conversion efficiency, this system ideally should produce 72 MWh (2480 × 0.16 × 182 m<sup>2</sup>) in a year under standard conditions (25 °C ambient temperature, 1 m/s wind speed). However, the 24 kW<sub>p</sub> Amonix HCPV in Phoenix, Arizona, generated a net of 49.2 MWh in 2005, a sizeable 30% difference (Herbert et al., personal communication). Losses associated with soiling, alignment, shadows between

units and other objects, temperature, equipment failures explain the discordance between the ideal and real performance.

## 7.2. Materials and energy balance

### 7.2.1. Materials and components production

The two-axis tracker and its foundation account for 58% of the 24 kW<sub>p</sub> Amonix concentrator system. The concentrator module (MegaModule), which includes frames, inside structure, Fresnel lenses, solar cells, and heat sinks, accounts for the next most significant contribution (41%). Steel is the material predominantly used for the HCPV system's heavy structures and equipment in the tracker and concentrator modules (Fig. 10). We calculated the energy demands and greenhouse-gas emissions during the manufacturing and assembly of the components that constitute Amonix HCPV systems, based on commercial and public databases (Table 5). Those processes encompassed are injection molding, contour shaping, wire drawing, pipe drawing, section-bar extrusion, solar-cell manufacturing, electronics manufacturing, and transportation of materials and parts.

### 7.2.2. Assembly and installation

The concentrator modules are assembled in manufacturing plant and transported to the field where other components are gathered, installed, and welded. After drilling a hole 1.2 m in diameter and 5.2 m deep, a 50-ton crane

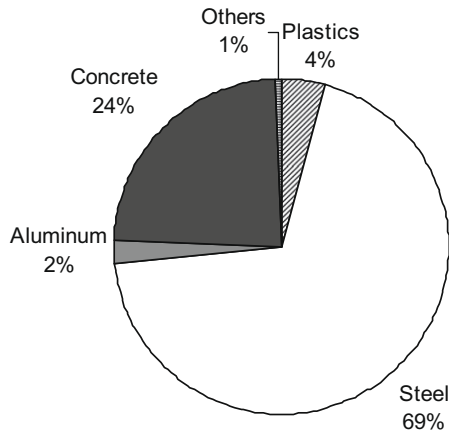


Fig. 10. Breakdown of materials used for the 24 kW, 21.3 metric ton Amonix HCPV system.

and a crew of four people place, assemble, and install the entire structure within half a day (Herbert et al., personal communication).

### 7.2.3. Maintenance and operation

We assumed that a monitoring and administrative office is built, as in a real, commercial application. Office energy use was estimated from a study on a PV BOS in the Tucson Electric flat-plate PV plant, Springerville, Arizona (Mason et al., 2006). A 2-hp pump runs intermittently for about an hour per day to track the sun during daytime under normal operations. It pulls about 1.4 kW, which translates into a daily parasitic energy use of 1.4 kWh (Herbert et al., personal communication).

### 7.2.4. End-of-life

The disposal of the Amonix HCPV components involves dismantling, transporting, and shredding them. We assumed that dismantling the components would require the same amount of energy as that used to install them. Also, we assumed that heavy trucks would transport the

dismantled components to a disposal facility 100 km away. Shredding and separating them will take 0.34 MJ/kg of energy (Staudinger and Keoleian, 2001). We considered the energy source for dismantling, transporting, and shredding those components to be diesel fuel.

### 7.3. Life-cycle metrics

Table 5 breaks down the primary energy demand during the life cycle of the 24 kW Amonix HCPV. The component manufacturing stage dominates the demand, accounting for 97% of the primary energy. Considering the 1.4 kWh/day of parasitic energy, the actual energy generated from this system is 48,700 kWh/year in Phoenix, which represents 605 GJ of primary energy avoided in using the primary to electric energy-conversion factor of 0.29 for the US average grid mix (Franklin Associates, 1998). This results in an EPBT of 1.3 years.

#### 7.3.1. Greenhouse-gas emissions

The greenhouse-gas (GHG) emissions during the life-cycle stages of the 24 kW<sub>p</sub> Amonix HCPV are estimated as an equivalent of CO<sub>2</sub> using an integrated time horizon of 100 years; they include CO<sub>2</sub>, CH<sub>4</sub>, N<sub>2</sub>O, and chlorofluorocarbons. Unlike fixed, standard PV configurations in which the emissions mostly are linked with manufacturing the solar cells, the tracking and concentrating equipment contributes the majority of the GHG emissions from this HCPV system. After normalizing for the electricity generated in Phoenix, 48,700 kWh/year, this system generates 38 g CO<sub>2</sub>-eq./kWh during its life cycle.

### 7.4. Discussions

Peharz and Dimroth recently investigated a FLATCON system that uses Fresnel lenses with a concentration rate of 500, with III–V multi-junction solar cells (Peharz and Dimroth, 2005). With an output power of 6 kW<sub>p</sub>, this system incorporates 333 individual triple-junction modules that have a DC conversion efficiency of 26%, which is 40% higher than the efficiency of the Amonix modules. The investigators calculated that the EPBT of the FLATCON system was about 0.7–0.8 years under operating conditions in Tabernas, Spain with direct solar radiation of 1900 kWh/m<sup>2</sup>/yr. This value corresponds to an EPBT of 0.5–0.6 years when adjusted to 2480 kWh/m<sup>2</sup>/yr of direct solar insolation with the 2-axis tracker observed in Phoenix (Table 6). This low EPBT is mainly attributed to the high efficiency of the triple-junction III–V solar cells. However, the stated annual electricity generation of the FLATCON system was not measured in the field; instead, it was estimated assuming an extremely low 6% loss of efficiency in cables and inverters, and no heating loss (Peharz and Dimroth, 2005). Furthermore, the authors did not fully account for losses in efficiency during field operation that stem from high wind, dust, maintenance, tracking errors, and cell-focus errors. After adjusting for them, the advantage that

Table 5  
Life-cycle primary energy demand and greenhouse-gas emissions (Kim and Fthenakis, 2006).

Stage	Energy (%)	GHG (%)
Components manufacturing		
MegaModule	58	54
Controller	0.5	0.3
Tracker	33	37
Electrical	2.3	1.8
Transportation	3.2	3.5
Office	0.3	0.4
Subtotal	97	97
Assembly and installation	0.1	0.2
Operation and maintenance	1.1	0.9
End-of-life disposal	1.7	1.9

Total primary energy = 817 GJ; total GHG = 56,000 kg CO<sub>2</sub>-eq. for a 24 kW<sub>p</sub> system.

Table 6  
Comparison of life-cycle parameters and performances across PV technologies (normalized for Phoenix insolation).

PV system	Amonix HCPV, 24 kW <sub>p</sub> current	Amonix HCPV, 24 kW <sub>p</sub> , future	Mono c-Si ground-mount*	CdTe ground-mount**
Module DC efficiency (%)	18	18	14	9
System loss (%)	32	17	20	20
Insolation (kWh/m <sup>2</sup> /yr)	2480 <sup>a</sup>	2480 <sup>a</sup>	2370 <sup>b</sup>	2370 <sup>b</sup>
EPBT (years)	1.3	1.1	1.8	0.8
GHG <sup>c</sup> (g CO <sub>2</sub> -eq./kWh)	38	31	35	18

\* Adapted from Alsema et al. (2005) and de Wild-Scholten and Alsema (2005).

\*\* Adapted from Fthenakis et al. (2005).

<sup>a</sup> Direct normal insolation with two-axis tracker.

<sup>b</sup> Longitude optimal insolation for flat-plate collectors.

<sup>c</sup> One hundred years of integrated time horizon.

a FLATCON system has over an Amonix system in terms of EPBT seemingly involves cell efficiency. With minimal adjustments, the Amonix system can be adapted to mount III–V solar cells. While this would reduce the EPBT, the decrease would not be proportional to the increased electricity generation since manufacturing multi-junction III–V solar cells involves many energy-intensive processes different from those in making single-crystal solar cells (Meijer et al., 2003).

The Amonix HCPV exhibits an advantage over the flat, fixed single-crystal silicon solar cell in terms of EPBT, but has a poorer performance for GHG emissions. This contrast between them mainly is related to the different energy sources for materials production. The cited studies of silicon solar cells assume that high-purity polycrystalline silicon, feedstock material for crystalline silicon ingots, is produced by a combined hydropower and gas-fired cycle (Alsema and de Wild-Scholten, 2005; de Wild-Scholten and Alsema, 2005). The Amonix HCPV incorporates a considerable number of steel structures the production of which consumes much energy from burning coal (Franklin Associates, 1998). However, by comparison, its life-cycle impact in terms of these two metrics is higher than that for thin-film CdTe PV at the same location (Table 6).

These findings must be interpreted cautiously as the Amonix systems are not produced or installed in a scale comparable to flat panel, Si- and CdTe-PV systems. Major components for the Amonix system including the Megamodules, trackers, and electrical equipment are yet to be optimized. The data for producing the single-crystal Si material for this system were taken from the literature, and the accuracy of the amount of electricity generated year round currently is being validated. Therefore, the present analysis may represent the life-cycle performance of a prototype, near commercial-version concentrator system, as distinct from the commercial PV modules.

## 8. Life-cycle risk analysis

### 8.1. Risk classification

Perhaps the greatest potential risks of the PV fuel cycle are linked with chemical usage during materials production and module processing (Hirschberg et al., 1998; Fthenakis, 2003). Although rare, accidents like leakage, explosion, and fire of toxic and flammable-substances are the major concerns to be addressed to ensure public acceptance of PV technology. But little is known about their frequency and scale in terms of human fatalities, injuries, and economic losses during the PV fuel cycle. In its burgeoning stage, the PV industry has not experienced major accidents of the same scale as other energy sectors. Furthermore, the stages of the PV fuel cycle are closely connected to the semiconductor processes that characterizing PV risks, i.e., equitably allocating risks to the PV and semiconductor industries poses many difficulties.

The risks associated with energy technologies can be classified into four types based on their scale, frequency, and the severity of harmful events (Fthenakis et al., 2006).

- (1) *Risk during normal operation-risks* of which the consequences are typically accepted, for example, GHG emissions, toxic chemical emissions, routine radioactive emissions, chemical/radioactive waste, and resource (fuel, water) depletion.
- (2) *Risk of routine accidents-risk* of accidents with high frequency and low consequences, for example, small-scale leakage of chemicals, small-scale explosion/fires, transportation accidents, and small-scale radioactivity release.
- (3) *Risk of severe accidents-risk* of accidents with low frequency and high consequences, for example, core meltdown, collapse of dam, and large-scale fire/explosion.
- (4) *Risk difficult-to-evaluate-risks* subject to, and sometimes reinforced by, perception. These include terrorist attacks on reactor/used fuel storage, geopolitical instability, military conflicts, energy security/national independence, and nuclear proliferation.

The first type of risk is characterized as routine under normal conditions as opposed to accidents, and their impact usually is limited by safety measures often established by regulation. This type of risk usually is determined by analytical tools, such as life-cycle analysis (LCA) and impact pathway analysis. The second and third types cover anomalous events or accidents. The general public is more concerned about the third type of risk, low-probability catastrophic events, than the second type, high-probability less severe accidents. The fourth type of risk is often associated with the public's perception, and the probability and consequences are difficult to evaluate (Haimes, 1998).

## 8.2. Risks of accidents in the PV life cycle

The greatest potential risks of the PV life cycle involve the toxic and flammable chemicals used for producing PV materials and for manufacturing modules (Fthenakis, 2003). Fthenakis and Kim undertook a life-cycle risk analysis based on accident records from a national database, the Risk Management Program (RMP). The study focused on the stages of handling and using the chemicals while making solar-cell materials and the modules (Fthenakis et al., 2006). The risks of potential accidents during installation, operation, and disposing/recycling PV modules may be negligible, as then, chemical usages are little or unnecessary.

According to the Clean Air Act Amendments of 1990, the US Environmental Protection Agency (EPA) is to publish regulations and guidance for facilities that use extremely hazardous substances to prevent chemical accidents. The US EPA developed the Risk Management Program Rule to implement the section 112 (r) of the amendments. This rule requires the facilities that produce, use, or handle toxic or flammable chemicals of concern in quantities over specific thresholds to submit a Risk Management Plan (RMP). Regulated substances and their threshold quantities are listed under section 112 (r) of the Clean Air Act in 40 CFR Part 68. The RMP should include a 5-year accident history detailing the cause of accidents and the damages to the employees, environment, and local public. Other RMP components include a hazard assessment for the most-likely and the worst-case accident scenarios, a prevention program covering safety precautions and maintenance, monitoring, and employee training measures, and an emergency response program that describes emergency

health care, employee training measures, and procedures for informing the public and response agencies (Environmental Protection Agency, 2002). In 1999, around 15,000 relevant facilities in the United States first submitted their accident records during the previous 5-year period, along with other documents. The current (2005) updated RMPs mostly cover accidents that occurred since mid-1999 for 17,000 country-wide facilities. The program must be resubmitted every 5 years and revised whenever there is a significant change in usage.

Fthenakis et al. estimated the risks of the chemicals used in the PV life cycle, i.e., accidents, fatalities, and injuries during the production, storage, and delivery of the flammable and toxic chemicals listed in 40 CFR Part 68, based on the current and past histories in the RMPs reported (Fthenakis et al., 2006). Table 7 shows the number of accidents/death/injuries between 1994 and 2004 for substances involved in PV materials and module production. Since there are very few data on the production/consumption of trichlorosilane ( $\text{SiHCl}_3$ ), estimates are given based on polysilicon production and capacity data. About 2 kg of polysilicon are needed to produce a module of  $6 \times 12$  cells of  $125 \text{ mm} \times 125 \text{ mm}$ , and an input of 11.3 kg of trichlorosilane is required to generate 1 kg of polysilicon (Alsema and de Wild-Scholten, 2005; Williams, 2000). No accidents were reported in the RMP database for phosphine and diborane in these years.

We note that the number of occurrences shown in Table 7 represents the total for all the US facilities that produce, process, handle, and store these chemicals in quantities over their specified thresholds. These statistics may include data irrelevant to the PV industry. For example, the majority (61%) of accidents/death/injuries attrib-

Table 7  
Incident records and estimated production for substances used in PV operation and regulated under the RMP rule.

Substance	Source	Total average (1994–2000) US production (1000 tonne/yr)	Number of incidents (employees and public) in the RMP database (1994–2004)		
			Incidents	Injuries	Deaths
<i>Toxic</i>					
Arsine ( $\text{AsH}_3$ )	GaAs CVD	23	2	1	0
Boron trichloride ( $\text{BCl}_3$ )	p-Type dopant for epitaxial silicon	NA	0	0	0
Boron trifluoride ( $\text{BF}_3$ )	p-Type dopant for epitaxial silicon	NA	1	1	0
Diborane ( $\text{B}_2\text{H}_6$ )	a-Si dopant	~50	0	0	0
Hydrochloric acid (HCl)	Cleaning agent for c-Si	3500	28	12	1
Hydrogen fluoride (HF)	Etchant for c-Si	190	165 (57) <sup>a</sup>	209 (70) <sup>a</sup>	1
Hydrogen selenide ( $\text{H}_2\text{Se}$ )	CIGS selenization	NA	4	17	0
Hydrogen sulfide ( $\text{H}_2\text{S}$ )	CIS sputtering	>110	40	47	1
Phosphine ( $\text{PH}_3$ )	a-Si dopant	NA	0	0	0
<i>Flammable</i>					
Dichlorosilane ( $\text{SiH}_2\text{Cl}_2$ )	a-Si and c-Si deposition	NA	2	0	0
Hydrogen ( $\text{H}_2$ )	a-Si deposition/GaAs	18,000 m <sup>3</sup>	57	65	4
Silane ( $\text{SiH}_4$ )	a-Si deposition	8	5	2	0
Trichlorosilane ( $\text{SiHCl}_3$ )	Precursor of c-Si	110	14	14	2

Sources: Williams (2000), EPA (1992), Census of Bureau (2002), Board on Environmental Studies and Toxicology (Best) (2003), U.S. Geological Survey (2003), Agency for Toxic Substances and Disease Registry (2004), and Pichel and Yang (2005).

<sup>a</sup> Number excludes incidents in petroleum refineries (NAICS 32411).

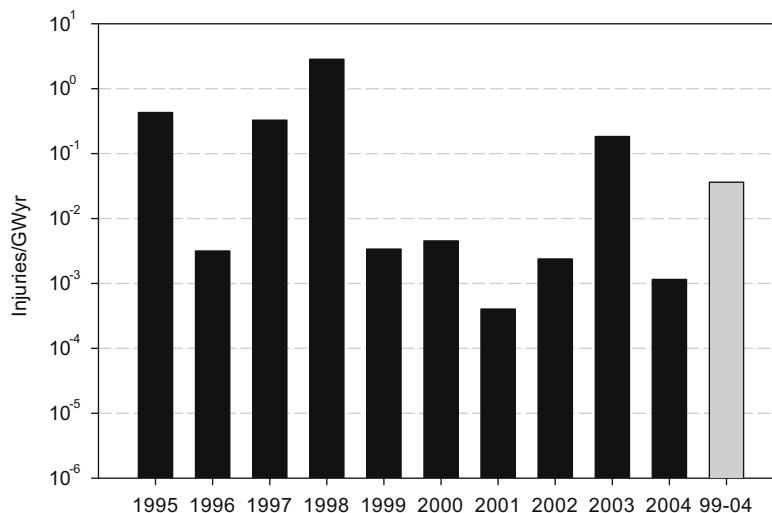


Fig. 11. Estimated injury rates of c-Si per GWyr electricity produced in the United States based on the year of accidents for HF, HCl, and SiHCl<sub>3</sub> (insolation = 1800 kWh/m<sup>2</sup>/year, performance ratio = 0.8).

uted to hydrogen fluoride (HF) occurred in petroleum refineries (NAICS<sup>4</sup> 32411), although refinery use accounts for only 6% of the US consumption (EPA, 1992). The petrochemical industry uses 100% HF under high pressure in large, multi-component units (e.g., alkylation units with many pipes, fittings, valves, compressors, and pumps) from where two-phase releases may occur, whereas the PV industry uses only aqueous solutions of HF (typically 49 wt%) in etching baths. Moreover, the usage of HF and hydrogen chloride (HCl) in the US PV industry accounts for less than 0.1% of the total in the United States. Therefore, we excluded HF use in the petroleum industries and the corresponding accidents from our analysis of risks in the PV fuel cycle.

To normalize the rate of accident/death/injuries, the figures are divided by the amount produced for those chemicals in the United States. The risks of each substance used in a 25 MW<sub>p</sub>/year scale PV industry are determined based on the amount of materials in Table 2. Then, the number of accidents/death/injuries per GWyr of electricity generated is determined as a risk indicator of chemical accidents in the PV fuel cycle based on the average US insolation of 1800 kWh/m<sup>2</sup>/year and a performance ratio of 0.8 (i.e., 20% system loss).

Fig. 11 depicts the rates of accidents/death/injuries for c-Si per GWyr electricity produced based on the average US insolation, 1800 kWh/m<sup>2</sup>/year. The last column with the most recent incident data (i.e., data submitted from 1999 onwards) may better represent the current evolution of the fast-growing PV industry. In general, for most chemicals, the numbers of accidents reported for the second cycle in the RMP (second half of 1999–2004) are lower than those reported in the first cycle (1994 to the first half of 1999). Specifically, only one accident involving silane

was reported during the second cycle of the RMP, whereas four accidents occurred during the first. Likewise, the number of accidents during the second RMP cycle involving trichlorosilane fell from 13 to 1 between 1994–1999 and 1999–2004. This across-the-board reduction of incidents likely represents improved safety in the whole US PV industry. For c-Si-PV modules, SiHCl<sub>3</sub>, the feedstock of polysilicon presents greater risks than other chemicals (Fig. 12). On the other hand, limited statistics suggest that silane poses the greatest risk in a-Si module manufacturing. The fatalities in Fig. 12 are related to HF. However, this risk is not based on the real events in PV facilities but is a virtual risk, derived from accident rates in other industries and the amount consumed in the PV industry. The real risk of HF in the PV industry, however, is likely to be lower than this current estimate due to the different characteristics of processes across industry sectors.

### 8.3. Comparison with other energy technologies

Fig. 13 compares fatality and injury rates across conventional electricity technologies and PV technologies. The figures for the conventional fuel cycles were extracted from the compilation of severe accident records of the GaBE project by the Paul Scherrer Institute (PSI), Energy-related Severe Accident Database (ENSAD) from 1969 to 2000 (Hirschberg et al., 2004). Although such a direct comparison may not be entirely appropriate, the data imply that the expected risks in the PV fuel cycle are lower than in other technologies, as we explain below. Thus, there are several caveats in directly comparing our estimate of PV risks and the risks estimated by the PSI's investigators. First, Hirschberg et al.'s assessments (2004) are based on severe accidents only, and small-scale accidents are ignored; the former are defined as events with at least 5 fatalities, 10 injuries, \$5 million of property damage, or

<sup>4</sup> North American Industry Classification System.

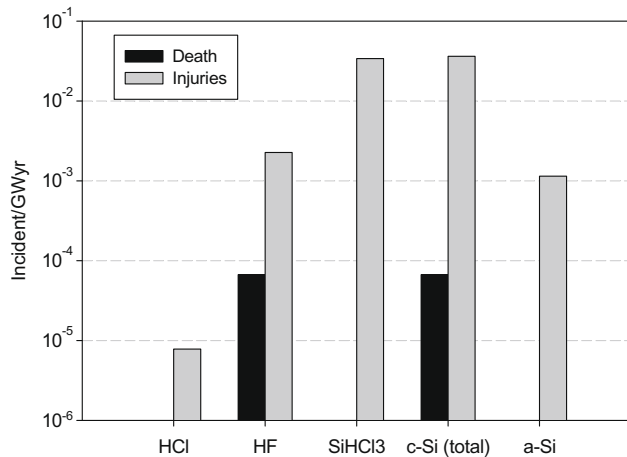


Fig. 12. Estimated incident rates by chemicals used between 1999 and 2004 (insolation = 1800 kWh/m<sup>2</sup>/year, performance ratio = 0.8). The rate of a-Si covers 1997–2004.

200 evacuees. On the other hand, only 20 out of the 318 incidents in Table 7 can be classified as severe accidents under the same definition. Therefore, the PSI's values for risk of conventional energy technologies may be underestimates. Also, we expect the safety records of the evolving PV industry to improve with time, whereas those for the mature conventional energy technologies are less likely to change. The risk estimate for the nuclear cycle in Fig. 13 relies on the probabilistic safety assessment (PSA) tool for the OECD countries rather than historical evidence due to insufficient experience related to the nuclear accidents. Although PSA is a logical approach to identify plausible accidents, their rates and consequences, it is not proven to provide absolute risk estimates due to its limita-

tions associated with data uncertainty; for example, risks of unexpected events or those triggered by human errors are impossible to fully account for (Linnerooth-Bayer and Wahlström, 1991; Nuclear Energy Agency, 1992). For the similar reason, the PSI's estimate for the PV cycle relied on data of the chemical industries handling similar substances used in the PV cycle (Peter et al., personal communication).

We also examined the maximum consequences of each energy technology. People are rarely neutral about risk; decision-makers, risk analysts, and the public are more interested in unforeseen catastrophes, such as bridges falling, dams bursting, and nuclear reactors exploding than in adverse, but routine events, such as transportation accidents. Comparing low-probability/high-damage risks with high-probability/low-damage events within one expected value frame often distorts the relative importance of consequences across technology options. Therefore, describing the maximum consequence potential makes sense (Haimes, 1998). Fig. 14 shows the maximum fatalities: figures for the fossil fuel and nuclear cycles are from a database (Hirschberg et al., 1998) and for PV from literature (Fthenakis et al., 2006; Hirschberg et al., 2004). From a scale of consequence perspective, PV technology is remarkably safer than other technologies. We anticipate that the maximum consequence will remain at the same level shown in Fig. 14 unless there is a significant change in PV production technologies.

The nature of risks varies with different energy technologies. The PSI analysis focuses on fuel mining, fuel conversion, power-plant operation, and transportation of fuels. On the other hand, fuel-related or power-plant-related risks are non-existent in the PV fuel cycle. Instead, our

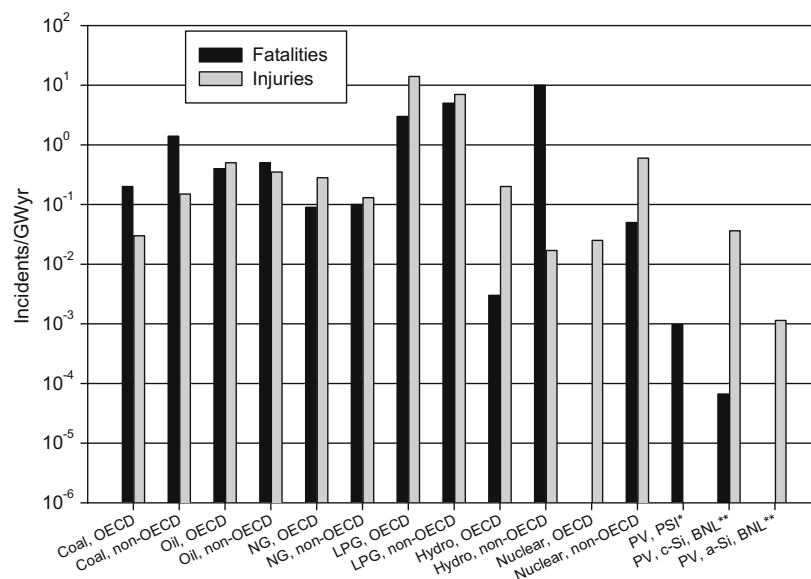


Fig. 13. Comparison of fatality and injury rates across electricity-generation technologies. The average US insolation = 1800 kWh/m<sup>2</sup>/year and a performance ratio = 0.8 was assumed. The incident rates for coal, oil, NG, LPG, hydro-, nuclear-, and PV technologies given by PSI are from Hirschberg et al. (2004) (NG, natural gas; LPG, liquefied petroleum gas; \* module type is not specified and injuries are not estimated; \*\* estimates of Brookhaven National Laboratory (BNL) based on US data (Fthenakis et al., 2006)).

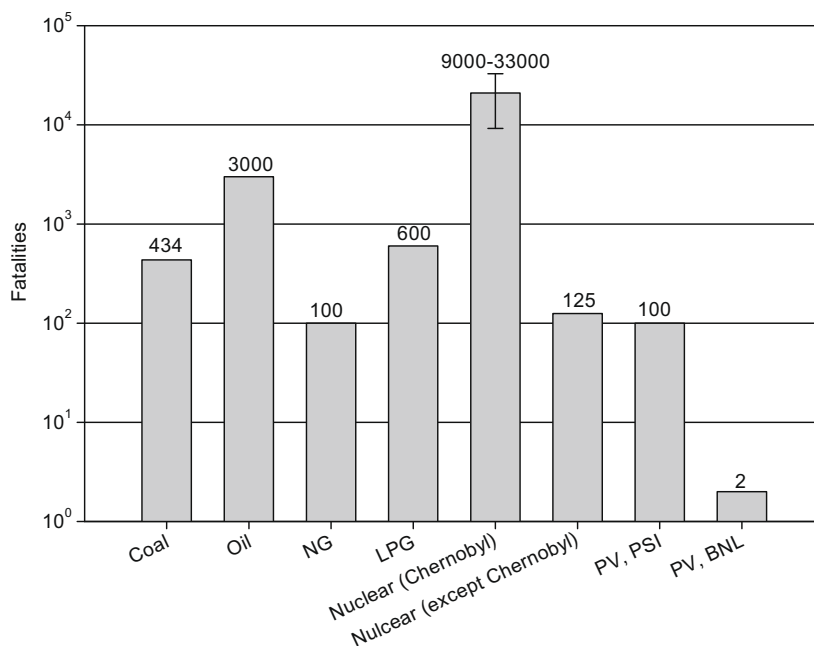


Fig. 14. Maximum fatalities from accidents across energy sectors. The number for Chernobyl includes latent fatalities. The incident rates for coal, oil, NG, LPG, hydro, nuclear, and PV given by PSI are from Hirschberg et al. (1998) (NG, natural gas; LPG, liquefied petroleum gas).

analysis of PV risks focuses on accidents associated with feedstock materials as well as process consumables, i.e., upstream risks, which the PSI analysis does not include.

#### 8.4. Limitation of study

As discussed, the hazards of trichlorosilane when making modules of c-Si, and of silane for a-Si modules have dominated concerns over other chemicals due to the large amount required and their flammability. Their limited number of incident records in the RMP database prevents our accurately measuring the safety of the PV industry. Since death records are very rare for these chemicals, the risk of fatalities is highly sensitive to a single incident. On the other hand, injury rates are relatively stable against the incremental number of injuries. This illustrates that the scale of the PV industry in terms of capacity and employees still is small so that such analyses are inadequate to directly compare with other technologies. PV technology still is in the early stage of commercial application, and, with time, Risk Management Programs compiled through experience eventually should stabilize the number of abnormal incidents. Other technologies, such as nuclear power, experienced a similar period during the early years of commercialization (Hirschberg et al., 1998).

Although PV technology is at an early stage compared with other energy systems, it is rapidly growing within the context of EU policy to increase the contribution of renewable energies to the total EU energy mix (Directive 2001/77/EC of the European Parliament and of the Council, 2001; European Commission, 1997). Accordingly, there are strong efforts to boost the PV sector, and therefore, it

should be treated more and more as an energy sector, avoiding comparisons with the chemical or semiconductor industry. Our analysis of risk in the PV life cycle is at a level lower than many other technologies. Given this situation, the PV industry should help by sharing information on risk, which, at the same time, could surely give PV more credibility and transparency.

## 9. Outlook

Alsema et al. (2006) recently outlined the major improvements in materials and energy consumption as well as conversion efficiencies which expected to be realized within a few years in the crystalline-Si PV sector. They forecast that the efficiency of ribbon-, multi-, and mono-Si module will improve to 15%, 17%, and 19%, respectively, in near future, in accordance with the target established by the Crystal Clear project. A fluidized bed reactor (FBR) currently being deployed will be able to reduce the energy demand for polysilicon by 70–90% from the popular Siemens process although it is unconfirmed if this new reactor type is capable of producing the same high-purity polysilicon as the latter (Alsema et al., 2006; Fthenakis and Kim, 2007a). At the same time, Si wafers will become thinner: 150  $\mu\text{m}$  for multi- and mono-Si and 200  $\mu\text{m}$  for ribbon-Si. Also, the energy demand during the casting of multi-crystalline ingots and the Czochralski growing of Si mono-crystal will fall as much as 3-fold (Alsema et al., 2006). The corresponding EPBT and GHG emissions are presented in Fig. 15.

We discuss the future of life-cycle GHG emissions from CdTe PV in a separate paper (Fthenakis and Kim, 2007a).

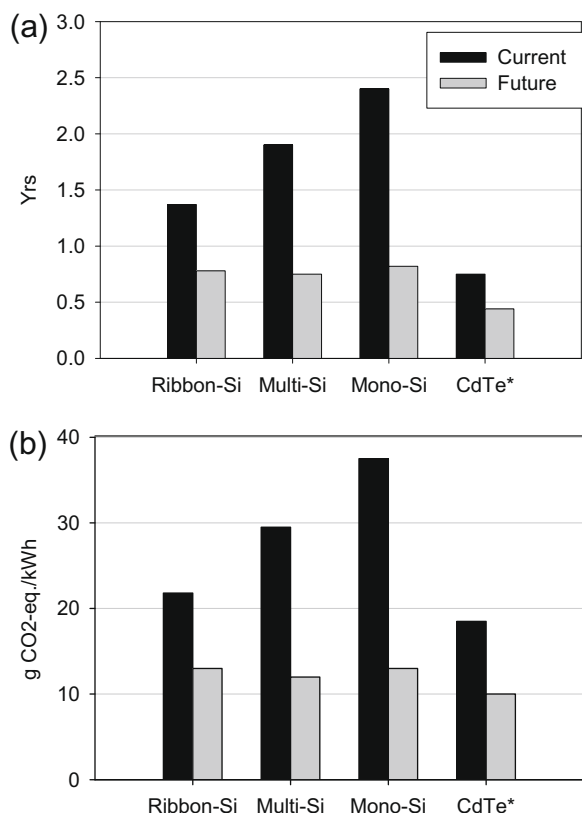


Fig. 15. Future forecast for (a) EPBT and (b) GHG emissions from the life cycles of PV modules (frame and BOS are not shown). Unless otherwise noticed, the estimates are based on the Southern European insolation, 1700 kWh/m<sup>2</sup>/year, a performance ratio of 0.75, and a lifetime of 30 years (\*Based on the average US insolation of 1800 kWh/m<sup>2</sup>/year and a performance ratio of 0.8).

The US manufacturer of CdTe PV predicts: (1) a linear increase in electrical-conversion efficiency from the current 9% to 12% by 2010; (2) a reduction of electricity requirements by about 25% within a couple of years through optimization of the deposition processes in CdTe lines; (3) about 20% of the manufacturing requirement will be satisfied via on-site solar electric generation. For a plant manufacturing 25 MW<sub>p</sub>/year of 12% efficient PV modules, the latest scenario will require a 1.3 MW<sub>p</sub> PV installation on 2.7 acres, which is area available on the roof and parking of the facility. Then, the EPBT would fall to 0.4 years and the GHG emissions to 10 g CO<sub>2</sub>-eq./kWh for the life cycle of installed CdTe PV under the average US insolation, 1800 kWh/m<sup>2</sup>/year (Fig. 15).

## 10. Conclusions

This review offers a snapshot of the rapidly evolving life-cycle performances of photovoltaic (PV) technologies and underlines the importance of timely updating and reporting the changes. During the life cycle of PV, emissions to the environment mainly occur from using fossil-fuel-based energy in generating the materials for solar cells, modules, and systems. These emissions differ in different countries,

depending on that country's mixture in the electricity grid, and the varying methods of material/fuel processing. The lower the energy payback times (EPBT), that is the time it takes for a PV system to generate energy equal to the amount used in its production, the lower these emissions will be. Under average US and Southern Europe conditions (e.g., 1700 kWh/m<sup>2</sup>/year), the EPBT of ribbon-Si, multi-crystalline Si, mono-crystalline Si, and CdTe systems were estimated to be 1.7, 2.2, 2.7, and 1.0–1.1 years, correspondingly. The EPBT of CdTe PV is the lowest in the group, although electrical-conversion efficiency was the lowest; this was due to the low energy requirement in manufacturing CdTe PV modules. We also report the potential environmental impacts during the life cycle of a 24 kW Amonix HCPV system which is being tested for optimization. The estimated EPBT of this system operating in Phoenix, AZ, is about 1.3 years and the estimated GHG emissions are 38 g CO<sub>2</sub>-eq./kWh. The EPBT of the Amonix mono-Si HCPV is shorter than that of a flat-plate mono-Si-PV ground-mount system, whereas GHG emissions are higher.

The indirect emissions of Cd due to energy used in the life cycle of CdTe PV systems are much greater than the direct emissions. CdTe PV systems require less energy input in their production than other commercial PV systems, and this translates into lower emissions of heavy metals (including Cd), as well as SO<sub>2</sub>, NO<sub>x</sub>, PM, and CO<sub>2</sub> in the CdTe cycle than in other commercial PV technologies. However, regardless of the particular technology, these emissions are extremely small in comparison to the emissions from the fossil-fuel-based plants that PV will replace.

The greatest potential risks of the PV fuel cycle are linked with the use of several hazardous substances, although in quantities much smaller than in the process industries. In an effort to measure the potential risks associated with the PV fuel cycle in comparison with other electricity-generation technologies, we used the US EPA's RMP accident records that cover the entire major US chemical storage and processing facilities. Our analysis shows that, based on the most recent records, the PV fuel cycle is much safer than conventional sources of energy in terms of statistically expected, and by far the safest in terms of maximum consequence. On the other hand, investigations are under way into the land and water uses during the PV fuel cycles in a comparative context, which is a relatively unknown territory of LCA (Koehler, 2008; Fthenakis et al., 2009).

Apparently, the PV industry is striving for cost savings simultaneously for advanced performance, which largely translates into life-cycle energy savings and emissions abatement. The conversion efficiency, material usage, and production energy efficiency of both Si and CdTe PVs are improving rapidly, thereby we also expect the risks associated with the life cycles of PV systems to be reduced. Frequent updates of these analyses are necessary to follow this evolution.

## References

- Agency for Toxic Substances and Disease Registry, 2004. Toxicological Profile for Hydrogen Sulfide.
- Alsema, E.A., 2000. Energy pay-back time and CO<sub>2</sub> emissions of PV systems. *Progress in Photovoltaics: Research and Applications* 8, 17–25.
- Alsema, E., de Wild-Scholten, M., 2005. Environmental impact of crystalline silicon photovoltaic module production. In: *Material Research Society Fall Meeting, Symposium G: Life Cycle Analysis Tools for “Green” Materials and Process Selection*, Boston, MA.
- Alsema, E.A., de Wild-Scholten, M.J., Fthenakis, V.M., 2006. Environmental impacts of PV electricity generation – a critical comparison of energy supply options. In: *21st European Photovoltaic Solar Energy Conference*, Dresden, Germany.
- Aulich, H.A., Schulze, F.-W., 2002. Crystalline silicon feedstock for solar cells. *Progress in Photovoltaics: Research and Applications* 10, 141–147.
- Australian Coal Industry Association Research Program (ACARP), 2004. *Coal in a Sustainable Society*.
- Board on Environmental Studies and Toxicology (BEST), 2003. *Acute Exposure Guideline Levels for Selected Airborne Chemicals*, vol. 3. The National Academic Press.
- Census of Bureau, 2002. *Current Industrial Reports – Inorganic Chemicals*. Available from: <<http://www.census.gov/manufacturing/cir/index.html>>.
- de Wild-Scholten, M., Alsema, E., 2005. Environmental life cycle inventory of crystalline silicon photovoltaic module production. In: *Material Research Society Fall Meeting, Symposium G: Life Cycle Analysis Tools for “Green” Materials and Process Selection*, Boston, MA.
- de Wild-Scholten, M.J., Alsema, E.A., ter Horst, E.W., Bächler, M., Fthenakis, V.M., 2006. A cost and environmental impact comparison of grid-connected rooftop and ground-based PV systems. In: *21st European Photovoltaic Solar Energy Conference*, Dresden, Germany.
- Directive 2001/77/EC of the European Parliament and of the Council, 2001. *Promotion of Electricity Produced from Renewable Energy Sources in the Internal Electricity Market*, 27 September, 2001.
- Dones, R. et al., 2003. *Sachbilanzen von Energiesystemen*. Final Report Ecoinvent 2000, vol. 6. Swiss Centre for LCI, PSI.
- Electric Power Research Institute (EPRI), 2002. *PISCES Data Base for US Power Plants and US Coal*.
- Environmental Protection Agency, 2002. *RMP Program Overview*. <<http://yosemite.epa.gov/oswer/Ceppoweb.nsf/content/RMPoverview.htm/>>, October 11th, 2002 (cited 22.02.07).
- EPA, 1992. *Hydrogen Fluoride Study*. Report to Congress. Office of Solid Waste and Emergency Response, US Environmental Protection Agency, Washington, DC.
- European Commission, 1997. *Communication from the Commission “Energy for the Future: Renewable Sources of Energy”*. White Paper for a Community Strategy and Action Plan.
- European Commission, 2003. *External Costs*. Directorate-General for Research, Office for Official Publications of the EC: Luxembourg, EUR 20198.
- Franklin Associates, 1998. *USA LCI Database Documentation*. Prairie Village, Kansas.
- Fthenakis, V., 2003. Overview of Potential Hazards. In: Markvart, T., Gastaner, L. (Eds.), *Practical Handbook of Photovoltaics: Fundamentals and Applications*. Elsevier.
- Fthenakis, V.M., 2004. Life cycle impact analysis of cadmium in CdTe PV production. *Renewable and Sustainable Energy Reviews* 8 (4), 303–334.
- Fthenakis, V., Alsema, E., 2006. Photovoltaics energy payback times, greenhouse gas emissions and external costs: 2004–early 2005 status. *Progress in Photovoltaics: Research and Applications* 14, 275–280.
- Fthenakis, V.M., Kim, H.C., 2005. Energy use and greenhouse gas emissions in the life cycle of CdTe photovoltaics. In: *Material Research Society Fall Meeting, Symposium G: Life Cycle Analysis Tools for “Green” Materials and Process Selection*, Boston, MA.
- Fthenakis, V.M., Kim, H.C., 2007a. Greenhouse-gas emissions from solar electric- and nuclear power: a life-cycle study. *Energy Policy* 35, 2549–2557.
- Fthenakis, V.M., Kim, H.C., 2007b. CdTe photovoltaics: Life cycle environmental profile and comparisons. *Thin Solid Films* 515, 5961–5963.
- Fthenakis, V.M. et al., 2005. Emissions and encapsulation of cadmium in CdTe PV modules during fires. *Progress in Photovoltaics: Research and Applications* 13, 713–723.
- Fthenakis, V.M. et al., 2006. Evaluation of risks in the life cycle of photovoltaics in a comparative context. In: *21st European Photovoltaic Solar Energy Conference*, Dresden, Germany.
- Fthenakis, V.M., Kim, H.C., Alsema, E., 2008. Emissions from photovoltaic life cycles. *Environmental Science & Technology* 42, 2168–2174.
- Fthenakis, V., Wang, W., Kim, H.C., 2009. Life cycle inventory analysis of the production of metals used in photovoltaics. *Renewable and Sustainable Energy Reviews* 13, 493–517.
- Fthenakis, V., Kim, H.C., 2009. Land use and electricity generation: a life-cycle analysis. *Renewable and Sustainable Energy Reviews* 13, 1465–1474.
- Garboushian, V., Roubideaux, G., Turner, G., Gunn, J.A., 1997. *Long-Term Reliability Concerns Resolved by Third Generation Integrated High-Concentration PV Systems*, 26th IEEE Photovoltaic Specialist Conference. Anaheim, CA.
- Haimes, Y.Y., 1998. *Risk Modeling, Assessment, and Management*, fourth ed. John Wiley & Sons.
- Hagedorn, G., 1992. *Kumulierter Energieaufwand von Photovoltaik und Windkraftanlagen*. Technischer Verlag Resch KG, München, Germany.
- Herbert, H., personal communication. Arizona Public Service.
- Hirschberg, S., Spikerman, G., Dones, R., 1998. *Severe Accidents in the Energy Sector*, first ed. Paul Scherrer Institute, Switzerland.
- Hirschberg, S. et al., 2004. *Sustainability of Electricity Supply Technologies under German Conditions: A Comparative Evaluation*. Paul Scherrer Institute, Switzerland.
- Hynes, K.M., Baumann, A.E., Hill, R., 1994. An assessment of the environmental impacts of thin-film cadmium telluride modules based on life cycle analysis. In: *IEEE 1st World Conference on Photovoltaic Conversion (WCPEC)*, Hawaii.
- Intergovernmental Panel on Climate Change, 2001. *Climate Change 2001: The Scientific Basis*. Cambridge University Press, Cambridge, UK.
- Jungbluth, N., 2005. Life cycle assessment of crystalline photovoltaics in the Swiss ecoinvent database. *Progress in Photovoltaics: Research and Applications* 13 (8), 429–446.
- Kato, K. et al., 2001. A life-cycle analysis on thin-film CdS/CdTe PV modules. *Solar Energy Materials & Solar Cells* 67, 279–287.
- Kim, H.C., Fthenakis, V.M., 2006. Life cycle energy demand and greenhouse gas emissions from an Amonix high concentrator photovoltaic system. In: *IEEE Fourth World Conference on Photovoltaic Energy Conversion*, Hawaii.
- Koehler, A., 2008. Water use in LCA: managing the planet’s freshwater resources. *International Journal of Life Cycle Assessment* 13, 451–455.
- Linnerooth-Bayer, J., Wahlström, B., 1991. Applications of Probabilistic Risk Assessments: The Selection of Appropriate Tools. *Risk Analysis* 11 (2), 239–248.
- Mason, J.E., Fthenakis, V.M., Hansen, T., Kim, H.C., 2006. Energy payback and life-cycle CO<sub>2</sub> emissions of the BOS in an optimized 3.5 MW PV installation. *Progress in Photovoltaics: Research and Applications* 14, 179–190.
- Maycock, P.D., 2005. *National Survey Report of PV Power Applications in the United States 2004*. International Energy Agency.
- Meijer, A. et al., 2003. Life-cycle assessment of photovoltaic modules: comparison of mc-Si, InGaP and InGaP/mc-si solar modules. *Progress in Photovoltaics: Research and Applications* 11 (4), 275–287.

- NREL, 1994. Solar Radiation Data Manual for Flat-Plate and Concentrating Collectors. National Renewable Energy Laboratory, Golden, CO.
- Nuclear Energy Agency, 1992. Probabilistic safety assessment: an analytical tool for assessing nuclear safety. In: NEA Issue Brief. Available from: <<http://www.nea.fr/html/brief>>.
- Palz, W., Zibetta, H., 1991. Energy pay-back time of photovoltaic modules. *International Journal of Solar Energy* 10, 211–216.
- Peharz, G., Dimroth, F., 2005. Energy payback time of the high-concentration PV system FLATCON. *Progress in Photovoltaics: Research and Applications* 13, 627–634.
- Peter, B., personal communication.
- Pichel, J.W., Yang, M., 2005. 2005 Solar Year-End Review & 2006 Solar Industry Forecast. Piper Jaffray & Co..
- Raugei, M., Bargigli, S., Ulgiati, S., 2007. Life cycle assessment and energy pay-back time of advanced photovoltaic modules: CdTe and CIS compared to poly-Si. *Energy* 32, 1310–1318.
- Rogol, M., 2005. Silicon and the solar sector: mapping a new world. In: Presentation at the Second Solar Silicon Conference, 11 April, 2005, Munich, Germany.
- Staudinger, J., Keoleian, G.A., 2001. Management of End-of-Life Vehicles (ELVs) in the US. Center for Sustainable Systems, University of Michigan.
- Swanson, R.M., 2003. Photovoltaic concentrators. In: Luque, A., Hegedus, S. (Eds.), *Handbook of Photovoltaic Sciences and Engineering*. John Wiley & Sons.
- U.S. Geological Survey, 2003. Mineral Commodity Summary: Arsenic.
- Williams, E., 2000. Global Production Chains and Sustainability: The Case of High-Purity Silicon and its Applications in IT and Renewable Energy. Institute of Advanced Studies, The United Nations University, Tokyo, Japan.
- Woditsch, P., Koch, W., 2002. Solar grade silicon feedstock supply for PV industry. *Solar Energy Materials & Solar Cells* 72, 11–26.

**Vasilis Fthenakis** is Senior Scientist and the Head of the Photovoltaics Environmental Research Center at Brookhaven National Laboratory in a joint appointment with Columbia University where he is a Professor of Earth and Environmental Engineering and the Founder and Director of the Center for Life-Cycle Analysis. He is the author of 200 publications, member of the Editorial Boards of *Progress in Photovoltaics* and the *Journal of Loss Prevention*. He also a Fellow of the American Institute of Chemical Engineers, a Fellow of the International Energy Foundation, and member of several energy and sustainability expert panels.

**Hyung Chul Kim** received his bachelor's and master's degrees from the Inorganic Materials Engineering at Seoul National University, and Ph.D. from the School of Natural Resources and Environment at the University of Michigan, Ann Arbor. In 2005, he joined the PV Environmental Research Center at the Brookhaven National Laboratory where he worked as a post doctoral research associate. Since May 2008, he has been working as an Associate Research Scientist in the Center for Life-Cycle Analysis at Columbia University. His research interests center on the LCA of products and energy systems including automobile, refrigerator, photovoltaics, and nuclear power. He also serves as a member of IEA's Technical Committee for Task 12, Environmental Health and Safety Issues of PV.